

ON THE FULL NON-GAUSSIAN SURPRISE STATISTIC AND THE COSMOLOGICAL CONCORDANCE BETWEEN DESI, SDSS AND PANTHEON+

PEDRO RIBA MELLO,^{1,2*} MIGUEL QUARTIN,^{1,3,4,5#} BJÖRN MALTE SCHÄFER,^{2,6} AND BENEDIKT SCHOSSER²

¹Instituto de Física, Universidade Federal do Rio de Janeiro, 21941-972, Rio de Janeiro, RJ, Brazil

²Zentrum für Astronomie der Universität Heidelberg, Astronomisches Rechen-Institut, Philosophenweg 12, 69120 Heidelberg, Germany

³Institut für Theoretische Physik, Universität Heidelberg, Philosophenweg 16, 69120. Heidelberg, Germany

⁴Observatório do Valongo, Universidade Federal do Rio de Janeiro, 20080-090, Rio de Janeiro, RJ, Brazil

⁵PPG Cosmo, Universidade Federal do Espírito Santo, 29075-910, Vitória, ES, Brazil

⁶Interdisziplinäres Zentrum für wissenschaftliches Rechnen, Universität Heidelberg, INF205, 69120 Heidelberg, Germany

Version August 19, 2024

ABSTRACT

With the increasing precision of recent cosmological surveys and the discovery of important tensions within the Λ CDM paradigm, it is becoming more and more important to develop tools to quantify accurately the discordance between different probes. One such tool is the Surprise statistic, a measure based on the Kullback-Leibler divergence. The Surprise, however, has been up to now applied only under its Gaussian approximation, which can fail to properly capture discordance in cases that deviate significantly from Gaussianity. In this paper we developed the `kl Surprise` code which computes the full numerical non-Gaussian Surprise, and analyse the Surprise for BAO + BBN and supernova data. We test different cosmological models, some of which the parameters deviate significantly from Gaussianity. We find that the non-Gaussianities, mainly present in the Supernova dataset, change the Surprise statistic significantly from its Gaussian approximation, and reveal a 2.7σ tension in the curved w CDM model (ow CDM) between the combined Pantheon+ and SH0ES (Pantheon+ & SH0ES) data and the dataset which combines SDSS, BOSS and eBOSS BAO. This tension is hidden in the Gaussian Surprise approximation. For DESI the tension with Pantheon+ & SH0ES is at the meager 1.9σ level for ow CDM, but a large 3.3σ for Λ CDM.

Subject headings: cosmology:observations – cosmological parameters – large-scale structure of Universe

1. INTRODUCTION

In the last 25 years cosmology has developed with great success over a well understood Λ CDM cosmological model. Over the last few years, however, a comparison of different probes have pointed to some important tensions in the model. In particular, the Hubble constant tension between the values preferred by the Planck satellite data of the Cosmic Microwave Background (CMB) (Planck Collaboration VI 2020) and Supernova observations calibrated locally with Cepheids from the SH0ES program (Riess et al. 2022), has been steadily increasing in significance and is now touching the 5σ threshold. This has motivated the community to look into alternative cosmological scenarios on the theory front, and possible systematics on the observational one.

In order to better study tensions, it is essential to quantify and describe them using different model frameworks. In fact, one must quantify the important question of what it means for two experiments to agree or disagree with each other. Many works have in this sense proposed different concordance and discordance estimators (CDE). These CDE's should not depend strongly on the functional forms analysed. Many of these rely

on the Bayesian evidence ratio \mathcal{B} between datasets (see, e.g., Verde et al. 2013; Martin et al. 2014; Raveri 2016). Hobson et al. (2002) discussed how \mathcal{B} can be used to suggest the need to add hyperparameters to a given model. Amendola et al. (2013) proposed an internal robustness test, which consists of a blind search for systematics by analysing \mathcal{B} for many random splits of a given dataset (see also Heneka et al. 2014; Sagredo et al. 2018). Some limitations of \mathcal{B} , such as the prior dependence was addressed in Handley & Lemos (2019); Amendola et al. (2024). See also Raveri & Hu (2019) for a review. The other ingredient needed for quantifying tensions is a scale, with which one compares the chosen metric. The Jeffrey scale is often employed as a way to compare Bayesian evidences for instance, but it has no fundamental basis and should be seen as empirical. The arbitrariness of Jeffreys' scale can be addressed by assuming a finite model space as discussed in Amendola et al. (2024) (see Castro & Quartin 2014, for an earlier example).

Another commonly used tool to assess agreement is the Kullback-Leibler divergence (KLD) Kullback & Leibler (1951), also called the relative entropy. It was used in March et al. (2011) to build a robustness metric which complements the traditional Figure-of-Merit. More recently, it was employed by Seehars et al. (2014) where it was used, together with the posterior predictive dis-

* peribamello@gmail.com

mquartin@if.ufrj.br

tribution (PPD, Huan & Marzouk 2013), to define the Surprise statistic S . It is a quantity which can be interpreted as an information gain from a newer experiment in regards to a previous one (Lindley 1956; Grandis et al. 2016). The idea is to compare the value S to its distribution, induced from the PPD, and thus compute a p -value statistics of the concordance hypothesis between the posteriors.

The KLD is asymmetric, so when comparing different probes which were not in a clear succession the choice of which is the new and which the previous dataset is not obvious. This asymmetry could be easily solved by symmetrizing both the KLD and the PPD. This would however has the disadvantage of losing the interpretation of information gain between probes, and doubling the (substantial) computational requirements for numerical evaluation. In fact, the computational cost can quickly become the limiting factor, not only for the Surprise but for many of the defined CDEs. Therefore, some simplifying assumptions are often made in the literature. For instance, one can workout analytical solutions for many CDEs assuming Gaussianity. Under the assumption that both likelihood distributions are Gaussian, that the model is a linear function of the parameters and that the priors are also Gaussian or uninformative, the resulting posterior is also Gaussian. This is referred to as the Gaussian Linear Model (GLM). Motivated by the fact that with current CMB data Gaussianity can be a good approximation within the Λ CDM model, Seehars et al. (2014) derived analytical expressions for the Surprise and circumvented the large computational requirements.

Initially the Gaussian solution for the Surprise statistic was applied to a historical sequence of CMB experiments showing a large Surprise between Wilkinson Microwave Anisotropy Probe (WMAP, Hinshaw et al. 2013) and the following Planck 2013 data release (Planck Collaboration XV 2014). Subsequently, Seehars et al. (2016) examined the Surprise statistic between WMAP and Planck 2015 (Planck Collaboration XIII 2016). Grandis et al. (2016) used the Surprise to quantify discordance between WMAP, Planck, BOSS and Supernova datasets in various cosmological models. A numerical method to evaluate the KLD was presented but the Surprise statistic distribution was evaluated using the Gaussian solution.

Although larger datasets tend to lead to smaller uncertainties, in general in science we are often testing whether new data is well described by the current paradigm or if new phenomena can be detected, often being described by new degrees of freedom. In the Bayesian context, adding more parameters often make non-Gaussianities larger due to the increase on the confidence intervals, and larger intervals tend to make deviations from linear approximations of the model more evident. This means that Gaussianity in the posteriors can be a constantly eluding goal. In cosmology, in particular, the deviations from Gaussianity in models beyond Λ CDM are clear for many different observables.

Different methodologies have been proposed to deal with the presence of non-Gaussianities in cosmological posteriors. One approach is to alleviate them by suitable transformation of variables (Schuhmann et al. 2016; Grandis et al. 2016), although these methods only Gaussianise the posteriors locally, not globally (Giesel et al. 2021). Another, is to use the DALI approximation

proposed by Sellentin et al. (2014), which consists of higher-order Fisher matrix approach. More recently, a method based on the partition function was also proposed in Röver et al. (2023).

For the Surprise statistic, however, these approximations have not been studied, so it remains to be seen whether they are appropriate. In fact, the Surprise is sensitive to the tails of the distributions, a region where the effects of non-Gaussianities is of less importance when considering the posteriors, since in that case the focus is usually on the high-density regions. Therefore evaluating the Surprise numerically without assuming approximate Gaussianity may be necessary to properly quantify discordances when using less constraining data and/or when considering models with more degrees-of-freedom than Λ CDM.

In this paper we aim to numerically evaluate the Surprise statistic and its distribution and to quantify how much it differs from the case where Gaussianity is assumed. We developed a fully numerical code to compute the Surprise, and apply it to 3 sets of baryonic acoustic oscillation (BAO) and supernova data, discussed below. We show that in most cases results differ substantially from the Gaussian calculations. We will consider models beyond the Λ CDM, and will devote particular attention to the ow CDM model, where both spatial curvature and the dark energy equation of state parameter w are left free to vary. We will also discuss the particular cases w CDM (oCDM), where we held as fixed values $\Omega_{k0} = 0$ ($w = -1$), as well as Λ CDM itself.

1.1. Analyzed Data

The Baryon Oscillation Spectroscopic Survey (BOSS, Alam et al. 2017) and Extended BOSS (eBOSS, de Sainte Agathe et al. 2019; Alam et al. 2021) were ground-breaking BAO surveys, which in some redshift ranges still contain the highest BAO precision. We will do a combined analysis of BOSS+eBOSS data, complemented at low-redshifts by 6dF (Beutler et al. 2011) and Sloan Digital Sky Survey (SDSS) DR7 galaxies (Ross et al. 2015). This combination was previously considered in Schöneberg et al. (2019); here we will refer to it simply as “BOSS+”. The Dark Energy Spectroscopic Instrument (DESI) survey (Aghamousa et al. 2016; Vargas-Magaña et al. 2018) is the next-generation step, and will produce a spectroscopic map covering 14000 deg² of the sky, covering the range $z = (0 - 1.6)$ with a combination of BGS, LRG and ELG galaxies (Adame et al. 2024a). The 2024 BAO data release (Adame et al. 2024b) has significantly extended the redshift coverage of BOSS, and subsequent data releases will far surpass the number of objects from BOSS. In terms of supernovae, the Pantheon+ catalog (Scolnic et al. 2022; Brout et al. 2022) contains 1550 different explosions and is among the most recent and extensive supernova catalogs. We will consider the Pantheon+ both with, and without the SHOES (Riess et al. 2022) calibration. In the latter case, H_0 cannot be constrained with supernova.

DESI collaboration results (Adame et al. 2024a,b) have shown that, in the Λ CDM model, there is a large tension of more than 3σ between Pantheon+ and DESI+BBN datasets. In that sense, we will apply both full and Gaussian Surprise statistic to evaluate the pairwise concor-

dance among these latest BAO and supernova datasets, extending the analysis to models beyond Λ CDM.

1.2. Choice of priors

For the ow CDM model, which is the most general model we consider, we adopt the following broad top-hat priors: $p(h) = \mathcal{U}[0.1, 1.2]$, $p(\Omega_{m0}) = \mathcal{U}[0.05, 1]$, $p(\Omega_{k0}) = \mathcal{U}[-1, 1]$ and $p(w) = \mathcal{U}[-3, -0.4]$. For the other models in which we fix Ω_{k0} and/or w , we leave the priors on the other parameters unchanged. We tested that even broader priors lead to no significant changes in our results.

2. COMPARING DISTRIBUTIONS AND THE SURPRISE STATISTIC

In this section we summarize the Surprise statistic and explore the numerical approaches to its calculation.

2.1. The Gaussian Surprise statistic

The Kullback-Leibler divergence provides a measurement of the difference between two posterior distributions $p(\Theta|\mathcal{D}_1)$ and $p(\Theta|\mathcal{D}_2)$.¹ It is a quantity borrowed from Information Theory, its axiomatically defined and reads:

$$D_{\text{KL}}[p(\Theta|\mathcal{D}_2)||p(\Theta|\mathcal{D}_1)] = \int d\Theta p(\Theta|\mathcal{D}_2) \log \left(\frac{p(\Theta|\mathcal{D}_2)}{p(\Theta|\mathcal{D}_1)} \right). \quad (1)$$

The relative entropy is given in units of the chosen logarithm base; in this specific case, natural units, or *nats*. A simple division by $\log 2$ converts nats into bits. The relative entropy works as a measure of discordance, as it is zero if, and only if, both distributions are the exactly equal. It is always positive and the larger its value, the more discordant the distributions are. It is also invariant under reparametrizations.

Since the KLD is an integration over the complete parameter space it incorporates all information present in both posteriors, and thus accounts for discrepancies in a more complete way than the usual metrics based on comparing marginalized posteriors. The KLD in the Gaussian case has a known analytical solution (Seehars et al. 2014, 2016):

$$D_{\text{KL}}^{\text{G}}[p_2||p_1] = \frac{1}{2} (\Theta_1 - \Theta_2)^T \Sigma_1^{-1} (\Theta_1 - \Theta_2) + \frac{1}{2} \left(\text{tr}(\Sigma_2 \Sigma_1^{-1}) - d - \log \frac{\det(\Sigma_2)}{\det(\Sigma_1)} \right), \quad (2)$$

where $p_1 \equiv p(\Theta|\mathcal{D}_1)$ and $p_2 \equiv p(\Theta|\mathcal{D}_2)$ are the posterior distributions from two different experiments, Θ_i are the best-fit values, Σ_i are the covariance matrices and d is the dimensionality of the parameter space. We also add an upper index G to any quantity for which we use its Gaussian approximation. Using equation (2) and considering the case of a one-dimensional Gaussian distribution, we see that a KLD value of 1 bit corresponds to a shift of about 1.18σ in central values or a reduction of 68% in standard deviation, and a p -value of 0.24.

¹ It is sometimes useful to define the KLD between the posterior and the prior (Kunz et al. 2006).

Although assuming Gaussianity can often be a reasonable approximation, there are many known exceptions in cosmology. This is particularly true for extensions of Λ CDM with a free dark energy equation of state parameter w . In particular, many cosmological models are significantly non-linear in the most often used parameters. Moreover, the constant search for new physics frequently entails adding extra weakly constrained parameters to the analysis. These, in turn, can lead to significant non-Gaussianities. In such cases, one can evaluate Eq. (1) numerically performing a Monte Carlo integration:

$$D_{\text{KL}}[p_2||p_1] = \frac{1}{N} \sum_{i=0}^N [\log p(\Theta_i|\mathcal{D}_2) - \log p(\Theta_i|\mathcal{D}_1)], \quad (3)$$

where $\{\Theta_i\}$ are samples from distribution $p(\Theta|\mathcal{D}_2)$.

In order to define a better motivated scale for the KLD and other relevant quantities, one can resort to the PPD, defined as:

$$p(\mathcal{D}_2|\mathcal{D}_1) = \int d\Theta p(\Theta|\mathcal{D}_1) \mathcal{L}(\mathcal{D}_2|\Theta). \quad (4)$$

The posterior predictive distribution gives a way to forecast the data distribution of a new experiment \mathcal{D}_2 taking as prior information the posterior $p(\Theta|\mathcal{D}_1)$ of a previous one. The PPD also has a closed analytical form when the likelihoods are Gaussian and the data is linear in its parameters. For a more general form of likelihoods and/or model, one can sample the PPD numerically by integrating Eq. (4) by Monte Carlo integration and using a preferred sampling method:

$$p(\mathcal{D}_2|\mathcal{D}_1) = \frac{1}{N} \sum_{i=0}^N \mathcal{L}(\mathcal{D}_2|\Theta_i), \quad (5)$$

where $\{\Theta_i\}$ are samples from the posterior $p(\Theta|\mathcal{D}_1)$. As the posterior predictive distribution is a function of data, it has the dimensionality of the dataset. For current type Ia supernovae (SN) catalogs, for instance, one can have a ~ 2000 dimensional function, which limits the choice of sampling strategies for the PPD. But considering that most likelihoods are well approximated by Gaussians, the sampling process can be made much simpler and thus feasible.

From the PPD, one can finally derive an expected value for the relative entropy D_{KL} by integrating Eq. (1) over all possible data realizations for \mathcal{D}_2 :

$$\langle D_{\text{KL}} \rangle = \int d\mathcal{D}_2 p(\mathcal{D}_2|\mathcal{D}_1) D_{\text{KL}}[p(\Theta|\mathcal{D}_2)||p(\Theta|\mathcal{D}_1)]. \quad (6)$$

The expected relative entropy also has an analytical solution for the GLM case, which is given by

$$\langle D_{\text{KL}}^{\text{G}} \rangle = -\frac{1}{2} \log \frac{\det \Sigma_2}{\det \Sigma_1} + \text{tr}(\Sigma_1^{-1} \Sigma_2). \quad (7)$$

With the definition of both the relative entropy and its expected value, Seehars et al. (2014) defined the Surprise statistic S as:

$$S = D_{\text{KL}} - \langle D_{\text{KL}} \rangle. \quad (8)$$

We note that the Surprise is related to the so-called Bayesian Complexity statistic \mathcal{C}_b as $S = -1/2 \mathcal{C}_b$ when

one takes p_1 to be the prior distribution (Kunz et al. 2006).

The Surprise S is a simple scalar and its distribution, by definition, has zero mean. The more positive S is, the more different both posteriors are. A negative S means that both posteriors are more compatible than statistically expected. Clearly, in order for the Surprise value to have any meaning, one must compare it to its expected distribution. This distribution is induced by the posterior predictive distribution and is the same as the KLD distribution up to a simple shift factor given by $\langle D_{\text{KL}} \rangle$. With S and its distribution, one can compute the statistical significance of the result. In particular, one can compute the p -value statistic. As shown in Seehars et al. (2014, 2016), if both likelihoods are Gaussian and the data is linear in the parameters, the Surprise and its distribution have an analytical solution, which is given by

$$S^G = \frac{1}{2} [\Delta\Theta^T \Sigma_1^{-1} \Delta\Theta - \text{tr}(\mathbb{1} \pm \Sigma_2 \Sigma_1^{-1})]. \quad (9)$$

Inside the trace term, the $-$ sign is used when \mathcal{D}_2 was used to update the posterior $p(\Theta|\mathcal{D}_1)$, while the $+$ sign is used when $p(\Theta|\mathcal{D}_2)$ was derived independently from \mathcal{D}_1 . The distribution of S follows a generalized χ^2 distribution and can be rewritten as a weighted sum of χ^2 variables Z_i with one degree of freedom, given by

$$\begin{aligned} S^G &= \frac{1}{2} \left(\sum_{i=1}^d \lambda_i Z_i - \text{tr}(\mathbb{1} + \Sigma_2 \Sigma_1^{-1}) \right) \\ &= \frac{1}{2} \sum_{i=1}^d \lambda_i (Z_i - 1), \end{aligned} \quad (10)$$

where λ_i are the eigenvalues of $\text{tr}(\mathbb{1} \pm \Sigma_2 \Sigma_1^{-1})$, d is the dimensionality of the parameter space and Z_i are random samples drawn from a χ^2 distribution. In what follows we will drop the superscript G to simplify the notation since it will be clear in context if we refer or not to the Gaussian approximation or the full expressions.

A few points are worth noting at this point. First, the expected value of the relative entropy in Eq. (6) depends only on the posterior $p(\Theta|\mathcal{D}_1)$ and on the likelihood $\mathcal{L}(\mathcal{D}_2|\Theta)$. If we also include the assumption of linearity between model and its parameters and Gaussianity of likelihoods, then the relative entropy in Eq. (7) depends only on the covariance matrices of the experiments. Therefore it is a quantity solely measuring the information gain update when performing a new experiment. The PPD in Eq. (4), which induces the value of $\langle D_{\text{KL}} \rangle$, is a prediction of the constraining power of the new experiments with regards to the old one (\mathcal{D}_1). This means that the PPD, will induce this distribution independent of the data collected in a new experiment \mathcal{D}_2 , and henceforth of the posterior $p(\Theta|\mathcal{D}_2)$.

Second, S is an asymmetric measurement due to both the asymmetry in the relative entropy given by Eq. (1) and the asymmetry in the PPD itself. Since it is also due to the PPD, it cannot be fully resolved by using as a distance metric the Bhattacharyya distance (Bhattacharyya 1946), which just like the KLD is a specific case for the Rényi entropy (see Pinho et al. 2021; Golshani & Pasha 2010), but unlike the KLD, is symmetrical. This

	h	Ω_{m0}	Ω_{k0}	w
Baseline mock	0.7	0.35	0.0	-1
New mock	0.7	0.34	-0.03	-1.03

TABLE 1
FIDUCIAL PARAMETERS OF OUR MOCK SUPERNOVA DATA.

asymmetry is a feature rather than a failure as further explored by Nicola et al. (2019). Due to this asymmetry S one must chose with care the order of the datasets \mathcal{D}_1 and \mathcal{D}_2 . An interpretation of the Surprise in the eyes of Information entropy is that the Surprise is measuring an information when going from posterior $p(\Theta|\mathcal{D}_1)$ to the posterior distribution $p(\Theta|\mathcal{D}_2)$. In that regards it makes sense that the we chose $p(\Theta|\mathcal{D}_1)$ to be less informative, or broader, than $p(\Theta|\mathcal{D}_2)$. Another interpretation could be that \mathcal{D}_1 comes from a previous experiment than \mathcal{D}_2 , like the analysis conducted in Seehars et al. (2014, 2016).

Finally, the choice of the KLD as the comparison term is not unique. The concept of using the PPD to induce a distribution of the metric-like quantity can be used in multiple forms. In Schosser et al. (2024) the same concept was applied in data-space using the Fisher matrix for instance. Another possible choice for a comparison quantity could be the Bayesian Evidence, but that requires the joint analysis of \mathcal{D}_2 and \mathcal{D}_1 . This is not a simple task when datasets are correlated or come from an update version of a previous experiment, like the analysis of DESI and BOSS+eBOSS data, which we will perform here. Also, the relative entropy has a clear interpretation in information theory as the updated information one gain from one experiment to another (Lindley 1956). This measures both the shift in precision and agreement between different probes. The PPD, on the other hand, measures the expected value of the relative entropy, which should also be interpreted as the expected shift in precision of the likelihoods. In that sense, the Surprise statistic can be interpreted as the information gain between probes and a measurement of agreement between them. Finally, we emphasise that both Surprise and KLD are very robust measures, and in particular work in cases where Gaussian measures fail. For instance, there is a well defined and finite KLD for Cauchy distributions.

2.2. Going beyond Gaussianity

In this section we evaluate the Surprise distribution using a fully numerical code and deviating from the GLM. The `klsurprise` code works by sampling the posterior predictive distribution as in equation (5), reconstructing a posterior distribution $p(\Theta|\mathcal{D}_2^i)$ for each PPD sample \mathcal{D}_2^i using Nested Sampling (Skilling 2004, 2006), and then performing the Monte Carlo integral in equation (3). The resulting vector will be used to reconstruct the distribution of D_{KL} , its mean value and consequently, the distribution of the Surprise, S . This distribution can then be then used with the value of the numerical Surprise statistic to compute a p -value. Appendix A describes the `klsurprise` code in detail.

It is important to note that although time consuming, for parameter spaces with a small number of dimensions the `klsurprise` code can be run on standard modern desktops. In fact for the case with $\mathcal{D}_1 = \text{BOSS+ \& BBN}$ and $\mathcal{D}_2 = \text{Pantheon+ \& SH0ES}$ in $ow\text{CDM}$, which has 4

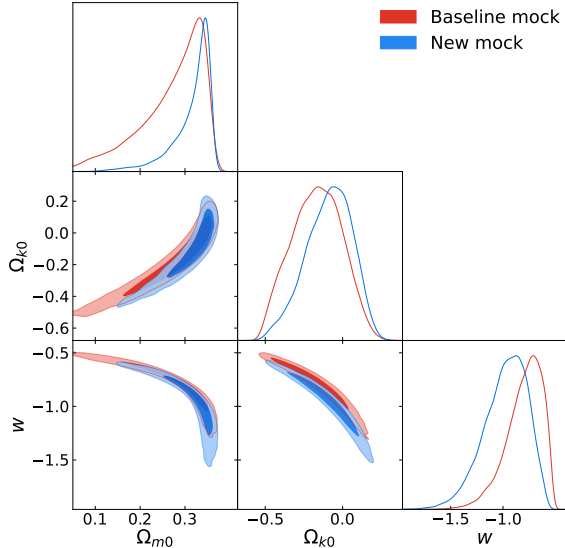


FIG. 1.— Marginalized 68% and 95% CI contour plots for our supernova mocks.

free parameters, the total computation time was a modest 540 CPU hours. This suggests that one does not need to rely on the Gaussian approximation on the grounds of computational cost alone, at least for small number of parameters.

2.3. Gaussian vs. non-Gaussian S

In Bayesian analysis, projection effects can create a false sense of agreement by failing to represent complex n -dimensional distribution in a one or two-dimensional plane. The Surprise statistic is a useful tool to identify such inconsistencies that might be hidden by marginalization projections. Consider for instance the illustrative example of two SN Ia mocks in a ow CDM model. Both were generated with a diagonal covariance matrix with a distance modulus error of $\sigma_\mu = 0.14$. The values of h are fixed in the likelihood analysis and the mocks fiducial parameters are given in Table 1.

The contour plots of the posterior distribution for these mocks are shown in Figure 1 and by themselves show no apparent large discordance between the datasets, as 2σ contours intersect. This consistency though, is only apparent, as the banana shaped contours of SN barely overlap when the contour plots are made in 3 dimensions, as shown in Figure 2. These hidden discordances can appear in multidimensional data and remain undetected when looking only at marginalized contours. The Surprise can account for these discrepancies, even for high dimensional data by translating the effective complexity of distributions into a one-dimensional distribution for S and also consequently a p -value statistics, which will indicate the probability for measuring a Surprise that deviates from zero by more than S . However, approximating the posterior distributions as Gaussians can sometimes make two disagreeing distributions to agree, as Gaussian approximations cannot fully describe the shape of some probability density functions.

For the specific case of the mocks constructed here, one can see that the Surprise deviate significantly from its linear Gaussian solution. The distribution of the Surprise

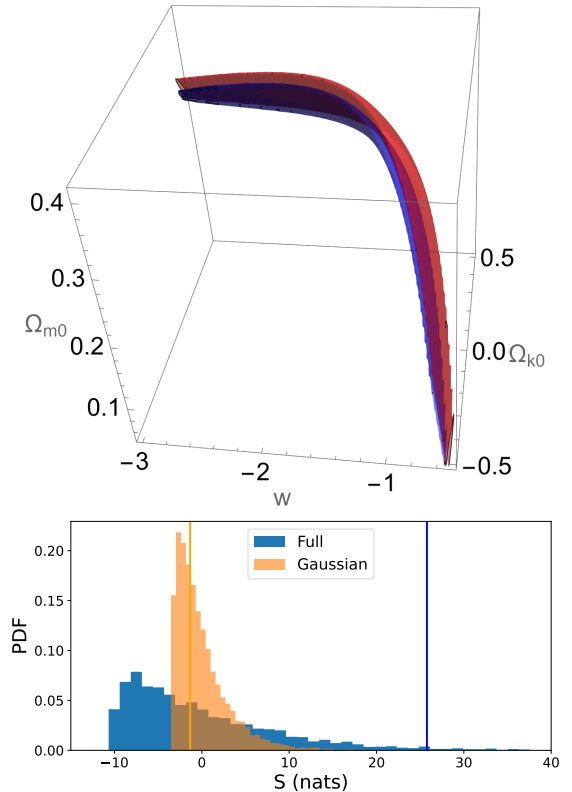


FIG. 2.— *Top*: three dimensional 95% confidence contour plots for SNIa mocks. *Bottom*: surprise statistic distribution for the mocks in Table 1.

is shown in Figure 2. The linear Gaussian solution for the Surprise distribution presents a much tighter distribution than that of the numerical Surprise. The relevant statistical quantities for this particular case can be seen in Table 2. Using the global covariance of the posterior to approximate them as Gaussians, effectively remove any discordances that could be fully appreciated in the full Surprise statistic. As can be seen from Table 2, the full result indicates a clear tension in datasets, while the analytical solution for the Surprise, which uses the GLM, does not.

3. DATA AND LIKELIHOODS

In this section, we present and discuss the datasets employed in our cosmological analysis using the non-Gaussian Surprise. Specifically, we examine the Pantheon+ & SH0ES SN Ia dataset (Riess et al. 2022; Brout et al. 2022) and the peak locations of Baryonic Acoustic Oscillations (BAO).

3.1. Pantheon+ Likelihood

The SNIa dataset employed in this study is sourced from Pantheon+ catalog. These supernovae span a redshift range from $z = 0.001$ to $z = 2.26$. The computation of the distance modulus incorporates calibrations based on Cepheid variable distances from the SH0ES collaboration Riess et al. (2022). The distance modulus is related to the luminosity distance as

$$\mu(\Theta|z) = 5 \log_{10} d_L(\Theta|z) + 25, \quad (11)$$

	Gaussian	Full
D_{KL}	2.80	36.4
$\langle D_{\text{KL}} \rangle$	4.03	10.6
S	-1.23	25.8
p -value	57.9%	2.6%
significance (σ)	0.55	2.27

TABLE 2
VALUES FOR THE SURPRISE STATISTIC BETWEEN TWO SNIa
MOCKS.

the luminosity distance d_L itself is a function of redshift and cosmological parameters (Hogg 1999).

The likelihood is built under the assumption of Gaussianity:

$$\mathcal{L}(\boldsymbol{\mu}|\Theta) = \frac{1}{\sqrt{(2\pi)^d |\boldsymbol{\Sigma}|}} \exp\left(-\frac{1}{2} \Delta\boldsymbol{\mu}^\top \boldsymbol{\Sigma}^{-1} \Delta\boldsymbol{\mu}\right), \quad (12)$$

where d is the dimensionality of the dataset $\Delta\mu_i = (\mu_i^{\text{obs}} - \mu_i(\Theta|z_i))$ and $\mu_i(\Theta|z_i)$ is the theoretical prediction for the distance modulus of the i^{th} SNIa in the catalog.

3.2. BAO+BBN Likelihood

For the analysis of BAO we utilized data from the BOSS+ combination. A comprehensive table of the data used for the BOSS+ likelihood is given in Table 3. The other likelihood utilized is from the DESI 2024 data release (Adame et al. 2024b), for which the dataset is given in Table 3. These datasets measure different distances at different redshifts. They are not used together, as they possess intercepting redshift bins, and therefore, non-zero correlations. To build the likelihood we use only the BAO peak locations, i.e., the redshift-dependent BAO scale ($1/Hr_s$), the angular BAO scale (D_A/r_s) and the volume averaged BAO scale (D_V/r_s). The DESI data has six different traces at different redshifts. The bright galaxy sample (BGS) are low redshift galaxies with z ranging from 0.1 to 0.4, the luminous red galaxy sample (LRG), the emission line galaxies (ELG) and Lyman- α (Ly α) tracers. In our analysis, a Gaussian likelihood is assumed for the data-vector and the cosmological background quantities, namely D_A , D_V , and H , are calculated using the Python package `jax-cosmo` (Campagne et al. 2023).

Given that the BAO likelihood exhibits degeneracy in the $H_0 - r_s$ plane, we employ Big Bang Nucleosynthesis (BBN) data as a prior for ω_b to estimate the sound horizon radius at the drag epoch, r_s . Although a Boltzmann code such as CLASS (Blas et al. 2011) is typically required for precise computation of r_s , we opted for a numerical approximation as in Aubourg et al. (2015):

$$r_s(z_d) \approx \frac{55.154 \exp[-72.3(\omega_b + 0.0006)^2]}{\Omega_{m0}^{0.25351} \omega_b^{0.12807}} \text{Mpc}, \quad (13)$$

where $\omega_X = \Omega_X h^2$, with $X = m, \nu, b$ for matter, neutrinos and baryons, and $H_0 = 100 h \text{ km/s/Mpc}$.

The Big Bang Nucleosynthesis (BBN) dataset leverages the abundance of deuterium to infer the density of baryons, given the correlation between these two quantities. Due to the absence of significant post-Big Bang production mechanisms for deuterium, its primordial abundance is deduced from observations of systems with low

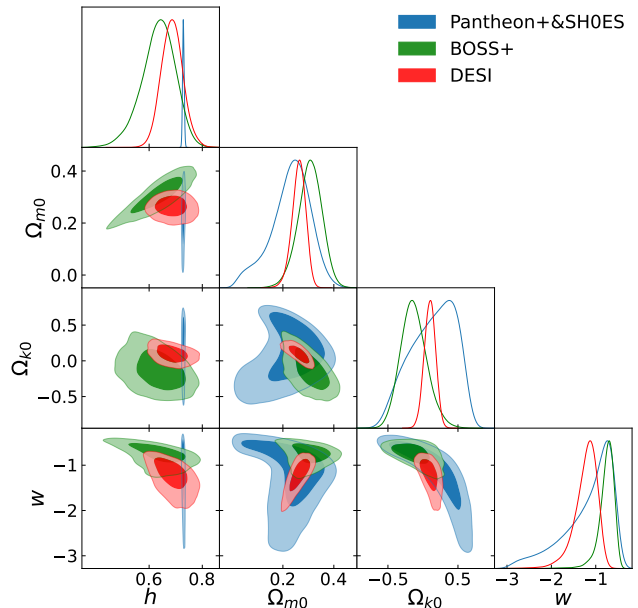


FIG. 3.— 1 and 2σ contours for the posteriors of DESI (red), BOSS+ (green) and Pantheon+ (blue) considering an ow CDM cosmological model.

metallicities (see Cyburt et al. (2016) for a review). These observations allow for the derivation of the baryon-to-photon ratio, η . Thus, observational constraints allow for the determination of primordial deuterium abundance and helium fraction, which can be used to deduce $\omega_b = \Omega_b h^2$. The constraints used for $\Omega_b h^2$ depend on the theoretical treatment of nuclear interaction cross-sections, mostly for the deuterium burning reactions. In this work, we use the predictions given in Schöneberg (2024), which make use of the code `PRyMordial` (Burns et al. 2024) and reports the constraints:

$$\omega_b = \Omega_b h^2 = 0.02218 \pm 0.00055. \quad (14)$$

4. NON-GAUSSIAN SURPRISE IN COSMOLOGY

As mentioned previously, we will adopt as our reference model the ow CDM model. In most models beyond Λ CDM, the dark energy equation of state parameter w is a time varying parameter. This is often taken into account using the simple CPL parametrization (Linder 2003; Chevallier & Polarski 2001), which adds a w_a parameter to account for this time-evolution of w . In many current cosmological probes, however, w_a is poorly constrained by the data, and thus the simpler model w CDM, with a fixed w , is used instead. Recent surveys such as DESI (Adame et al. 2024b) have shown, when combined with supernova data, hints of a nonzero w_a , putting a new tension in the standard Λ CDM scenario, although results are still heavily influenced by the choice of prior (Cortés & Liddle 2024). Since here our focus is to analyze the Surprise between pairs of probes without combining them, we choose to focus on the ow CDM, without including w_a .

Figure 3 shows the 1 and 2σ contours in the ow CDM model for the main datasets here considered: BOSS+, DESI and Pantheon+ & SH0ES. On inspection of this

	z_{eff}	D_M/r_d	D_H/r_d	D_V/r_d or r
BOSS+				
6DF	0.106	—	—	$r_d/D_V = 0.327 \pm 0.015$
SDSS DR7 MGS	0.15	—	—	4.47 ± 0.16
SDSS DR14 eBOSS QSO	1.52	—	—	26.0 ± 1.0
SDSS DR12 BOSS galaxies	0.38, 0.51, 0.61	full covariance	full covariance	—
SDSS DR14 eBOSS Ly- α	2.34	37.41 ± 1.87	8.86 ± 0.29	—
DESI				
BGS	0.30	—	—	7.93 ± 0.15
LRG	0.51	13.62 ± 0.25	20.98 ± 0.61	$r = -0.445$
LRG	0.71	16.85 ± 0.32	19.90 ± 0.51	$r = -0.420$
LRG+ELG	0.93	21.71 ± 0.28	17.88 ± 0.45	$r = -0.389$
ELG	1.32	27.79 ± 0.69	13.82 ± 0.42	$r = -0.444$
QSO	1.49	—	—	26.07 ± 0.67
Ly α QSO	2.33	39.71 ± 0.94	8.52 ± 0.17	$r = -0.477$

TABLE 3

COMPREHENSIVE LIST OF THE BAO DATA USED. *TOP*: THE BOSS+ COMBINATION: 6dF + SDSS BOSS + eBOSS. *BOTTOM*: DESI. NOTE THAT FOR EACH SAMPLE WE MEASURE EITHER BOTH D_M/r_d AND D_H/r_d , WHICH ARE CORRELATED WITH A COEFFICIENT r , OR D_V/r_d .

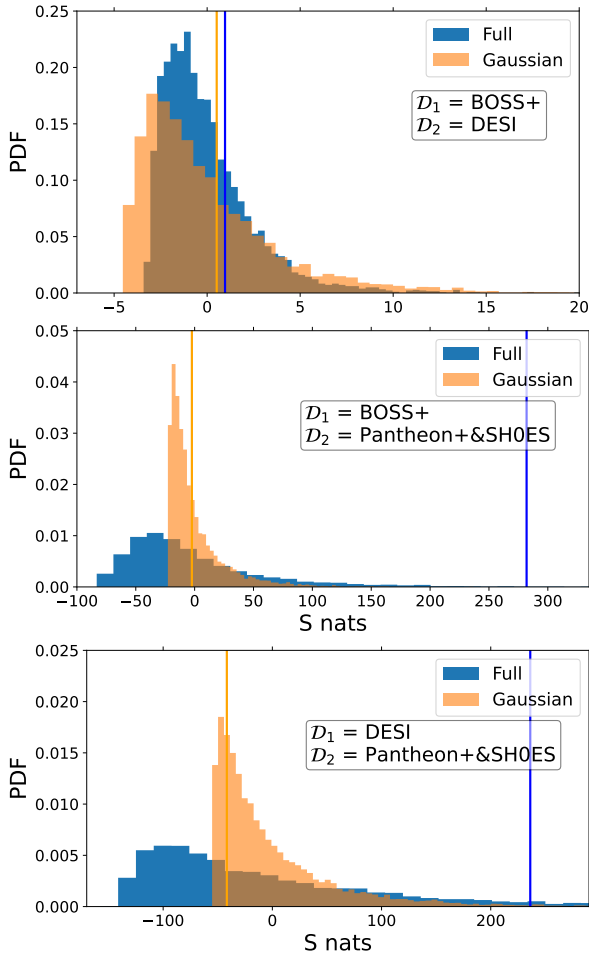


FIG. 4.— Surprise distribution for the ow CDM model, for the analytical Gaussian approximation (orange) and full numerical solution (blue). The vertical lines represent the actual Surprise values. *Top*: DESI as \mathcal{D}_2 , BOSS+ as \mathcal{D}_1 . *Middle*: Pantheon+ as \mathcal{D}_2 , BOSS+ as \mathcal{D}_1 . *Bottom*: Pantheon+ as \mathcal{D}_2 , DESI as \mathcal{D}_1 . We note tensions between Pantheon+ & SH0ES and DESI/BOSS+ probes (see also Table 5). Moreover, the Gaussian S is not a good approximation when using supernovae. DESI and BOSS+ data instead seem to agree with each other and the Gaussian S is a good approximation.

Figure, DESI seems reasonably Gaussian, whereas some non-Gaussianity is present in BOSS+ and considerable non-Gaussianities are apparent on Pantheon+ & SH0ES. This hints at the fact that while a Surprise analysis of purely BAO data assuming Gaussianity may lead to reasonable results, if one involves the supernova data S must be computed using the full numerical treatment.

Figure 4 illustrates the different distributions for S assuming the ow CDM model, for both the full numerical solution and the Gaussian approximation. We show the three possible combinations of datasets. One can see that, as expected, the surprise between both BAO datasets can be reasonably approximated by its Gaussian solution. However, large deviations from the simple Gaussian solution when the supernova data is considered. We will discuss this in more detail below for each pair of data.

4.1. DESI vs. BOSS+

One of the main advantages of the Surprise is that it can be used with correlated experiments without the need to perform a joint analysis. In that sense, an obvious use of the Surprise is to compare DESI and BOSS+ experiments. In this particular case, the asymmetry of the Surprise distribution naturally leads us to consider as BOSS+ as a previous experiment to DESI. I.e., it's natural to use $\mathcal{D}_1 = \text{BOSS+}$ and $\mathcal{D}_2 = \text{DESI}$. For these two datasets in a ow CDM model, both the analytical and the numerical results for the Surprise indicate no apparent tension, as can be seen from results in Table 4. The validity of the Gaussian S can be seen in the top panel of Figure 4 and also in the results of Table 4.

The analysis of the Surprise between BOSS+ and DESI show no apparent tension. It is worth noting that BOSS+ and DESI data have non-zero correlations, as they measure intersecting volumes. In the full analysis, DESI data shows a tension at the 3σ level between data in the redshift range of $0.6 < z < 0.8$ in Λ CDM. This tension, however, disappears with the addition of other data points. In fact, no tension is present in any of the cosmological models here analysed, as depicted in Figure 5. The tension computed from the Surprise barely surpasses the 1σ value, indicating a good cosmological agreement between BOSS+ and DESI.

	DESI BOSS+		Pantheon+ DESI	
	Gaussian	Full	Gaussian	Full
D_{KL}	5.25	5.61	62.0	51.9
$\langle D_{\text{KL}} \rangle$	5.21	4.28	102.8	46.6
S	0.04	1.33	-40.8	5.36
p -value	35.0%	22.4%	77.7%	26.2%
significance (σ)	0.93	1.22	0.28	1.12

TABLE 4

VALUES FOR THE SURPRISE STATISTIC $S(\text{DESI}|\text{BOSS}+)$ AND $S(\text{PANTHEON}+|\text{DESI})$, BOTH IN A $ow\text{CDM}$ COSMOLOGICAL MODEL.

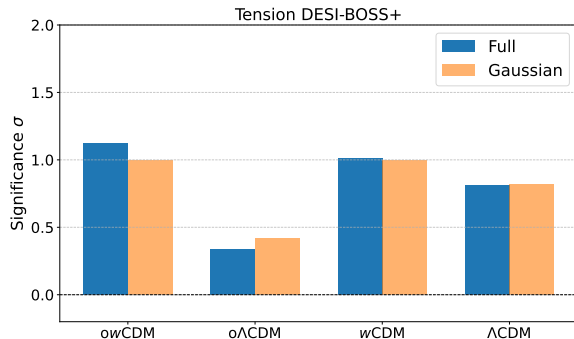


FIG. 5.— Tension in σ considering $\mathcal{D}_1 = \text{BOSS}+$ and $\mathcal{D}_2 = \text{DESI}$. The tension was evaluated by computing the significance of the p -value from the Surprise statistic and its distribution for different cosmological models.

4.2. The tension between Pantheon+ and BAO+BBN.

We now consider the Surprise between the supernova and BAO+BBN datasets. We will consider $\mathcal{D}_1 = \text{DESI}$ or $\text{BOSS}+$ and $\mathcal{D}_2 = \text{Pantheon+} \& \text{SH0ES}$. The BBN prior of ω_b is applied and marginalized over in the BAO+BBN likelihood so the parameter space is restricted to a common set of parameters for both experiments.

Table 5 below summarizes the surprise for all four cosmological models here considered ($ow\text{CDM}$, $o\text{CDM}$, $w\text{CDM}$, ΛCDM), and for both the full numerical S and its Gaussian approximation. In what follows we will discuss the results for each cosmological model separately.

4.2.1. S for the $ow\text{CDM}$ model

We analyse first the full $ow\text{CDM}$ model, since it is the one with the most degrees of freedom. The $ow\text{CDM}$ model also offers the best insight on the behaviour of the non-Gaussian Surprise, as the data is a highly non-linear function of the parameters and the contour plots deviate significantly from Gaussianity, as can be seen in Figure 3. In fact, again as expected the Surprise distribution deviates significantly from the solution assuming the Gaussian linear model, as can be seen in the bottom panel of Figure 4.

For the case where $\mathcal{D}_1 = \text{BOSS}+$ the full solution for the Surprise finds a p -value of 0.7%, indicating a tension between the datasets. This tension appears in the 4-dimensional parameter space, but most of its contribution comes from the known H_0 tension. We can visualize the contour plots in 3-dimensions by marginalizing over Ω_{m0} to try and understand the origins of the tensions. This is depicted in Figure 6. We see that in the $\{h, \Omega_{k0}, w\}$ space there is a very limited intersection be-

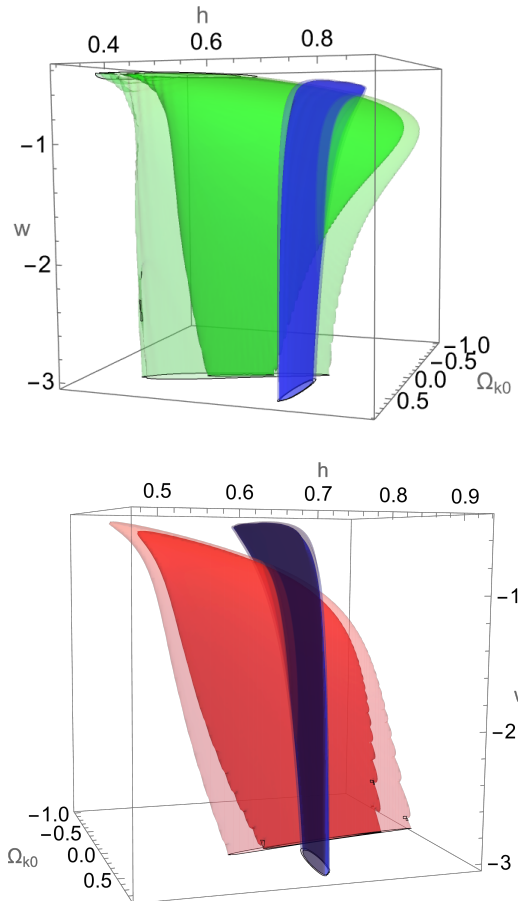


FIG. 6.— 3D posteriors contour plots of 68% and 95% CI. *Top*: Pantheon+ & SH0ES (blue) and BOSS+ posterior (green), marginalizing over Ω_{m0} . *Bottom*: Pantheon+ & SH0ES (blue) and DESI (red), marginalizing over H_0 .

tween the posterior PDFs, causing high values of the relative entropy between both distributions and, therefore, a high value of S . This explains the discordance between seen in the top panel of Table 5.

When analysing the same model, but considering DESI as our \mathcal{D}_1 , the p -value increases to 5.8%, which is still a slight indication of a tension. The Surprise distribution for this case still deviates significantly from the GLM (bottom panel of Figure 4). Both the expected relative entropy and the relative entropy have significantly different values than their counterpart solutions in the GLM.

Again, we can analyse the contour plots in the 3D $\{h, \Omega_{k0}, w\}$ space as seen in Figure 6 to see where the discrepancy of DESI and Pantheon+ data comes from. We see that the contour plots of DESI shrink significantly in relation to BOSS+. This causes the overlap between the distribution to increase in relation to the total distribution mass, which causes a decrease in the value of the Kullback-Leibler divergence and thus the Surprise. The distributions however, present a slight tension of 1.9 σ significance.

To illustrate that most of the tension between the two data-sets comes from the SH0ES and BBN priors, we made one further test. When computing the distribution of the Surprise, one can marginalize the posteriors over the parameter h before computing the Kullback-

	owCDM		oΛCDM		wCDM		ΛCDM	
	Gaussian	Full	Gaussian	Full	Gaussian	Full	Gaussian	Full
BOSS+ vs. Pantheon+ & SH0ES								
D_{KL} (nats)	37.8	392.7	67.6	88.1	88.1	180	7.19	7.14
$\langle D_{\text{KL}} \rangle$ (nats)	39.7	113	36.3	44.8	57.5	112	3.82	3.34
S (nats)	-1.88	280	31.3	43.2	30.6	67.8	3.37	3.8
p -value	36.1%	0.7%	9.4%	10.0%	14.7%	17.4%	5.9%	5.5%
significance (σ)	0.91	2.70	1.67	1.64	1.45	1.36	1.89	1.92
DESI vs. Pantheon+ & SH0ES								
D_{KL} (nats)	63.8	437.9	112.6	137.6	86.9	227	18.7	18.4
$\langle D_{\text{KL}} \rangle$ (nats)	107.0	197.5	59.0	71.1	57.2	71.2	3.6	3.3
S (nats)	-43.2	240.4	53.7	66.5	29.7	155.8	15.2	15.1
p -value	78.3%	5.8%	8.7%	10.3%	15.0%	6.0%	0.10%	0.10%
significance (σ)	0.27	1.90	1.71	1.63	1.44	1.88	3.32	3.35

TABLE 5

RESULTS FOR THE $S(p(\Theta|\mathcal{D}_2) | p(\Theta|\mathcal{D}_1))$ FOR BOTH GAUSSIAN APPROXIMATION AND THE FULL NUMERICAL RESULT, FOR DIFFERENT COSMOLOGICAL MODELS. HERE \mathcal{D}_1 IS EITHER BOSS+ OR DESI (BAO+BBN) AND \mathcal{D}_2 IS PANTHEON+ & SH0ES. WE MARK IN RED VALUES WITH SIGNIFICANCE ABOVE 2σ .

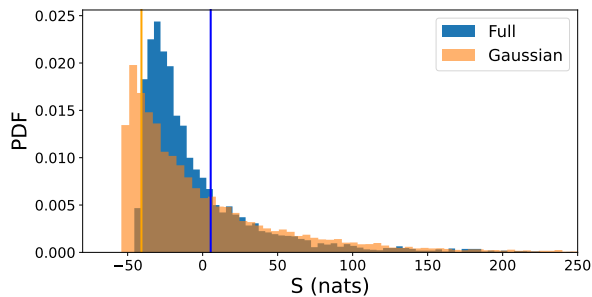


FIG. 7.— Similar to Figure 4c but now dropping BBN and SH0ES, and thus without the H_0 degree of freedom. $\mathcal{D}_1 = \text{DESI}$ and $\mathcal{D}_2 = \text{Pantheon+}$.

Leibler divergence. This isolates the posterior from the effects of the SH0ES and BBN priors and provides a distribution of the Surprise without the parameter h , as can be seen in Figure 7. In this particular parameter space $\{\Omega_m, \Omega_k, w\}$, Pantheon+ and DESI are in agreement with a p -value of 26.2%, indicating the tensions indeed comes mostly from h . The results for the Surprise marginalizing h are presented in Table 4, both for the full Surprise result and the analytical solution in the GLM.

In summary, BOSS+ and DESI have no significant tension, BOSS+ & BBN and Pantheon+ & SH0ES have a 2.7σ tension, DESI+BBN and Pantheon+ & SH0ES have a slight 1.9σ tension. Marginalizing results over h , we find that this slight tension between DESI and Pantheon+ disappears. This means that the tension in data is, unsurprisingly, introduced by the tension in h .

4.2.2. S for the oΛCDM model

A notably common extension of the ΛCDM model is the oΛCDM, which possesses a non-vanishing curvature parameter Ω_{k0} . The contour plots of the distributions in the top-left panel of Figure 8 show some resemblance to Gaussian distributions, the values for relative entropy in Table 5 suggest a slight deviation from Gaussianity, but less pronounced than in previous examples such as the owCDM case. The numerical result for the Surprise distribution shown in the bottom-left panel of Figure 8 deviates less from the analytical solution of the Surprise, shown in orange.

Besides the differences between the analytical and the

numerical solution, the p -value indicates a similar significance between the results and indicate no tensions between neither BOSS+ or DESI and Pantheon+ & SH0ES.

4.2.3. S for the wCDM model

In this model both all posterior distributions show clear signs of non-gaussian behaviour, as can be seen in the top-right panel of Figure 8.

Their respective values of relative entropy, as can be seen in Table 5, are considerably different from their Gaussian counterparts. The BOSS+ datasets presents no tension and is in agreement with the Pantheon+ & SH0ES dataset, both when considering the numerical and analytical Surprise statistics. The DESI dataset however presents a slight disagreement, with a p -value of 6%, which is a tension of approximately 1.88σ . This slight tension is only present when considering the full solution for the Surprise, and it is dissipated by the analytical treatment of the Surprise.

4.2.4. S for the flat-ΛCDM model

The flat-ΛCDM (ΛCDM) model possesses no curvature and a cosmological constant, whose eos parameter is $w = -1$. In the FACDM model the posterior distributions are very well approximated by Gaussians, as can be seen by the results in Table 5. The numerical distribution for the Surprise is the same as the analytical one and the Gaussian Linear Model is a good approximation in this case. In this case, the Surprise points towards a slight tension of around 1.9σ between $\mathcal{D}_2 = \text{Pantheon+ & SH0ES}$ and $\mathcal{D}_1 = \text{BOSS+ & BBN}$. If we choose $\mathcal{D}_1 = \text{DESI+BBN}$, however, there is a significant tension with a p -value of 0.1%, this p -value corresponds to a 3.3σ tension between datasets.

5. CONCLUSIONS

Analyzing the Surprise statistic beyond its Gaussian approximation provides a more robust analysis of the tensions between various cosmological probes. We find significant deviations from the Gaussian approximation, particularly when considering models beyond the standard ΛCDM framework and using supernova data. We demonstrated with a mock data example how

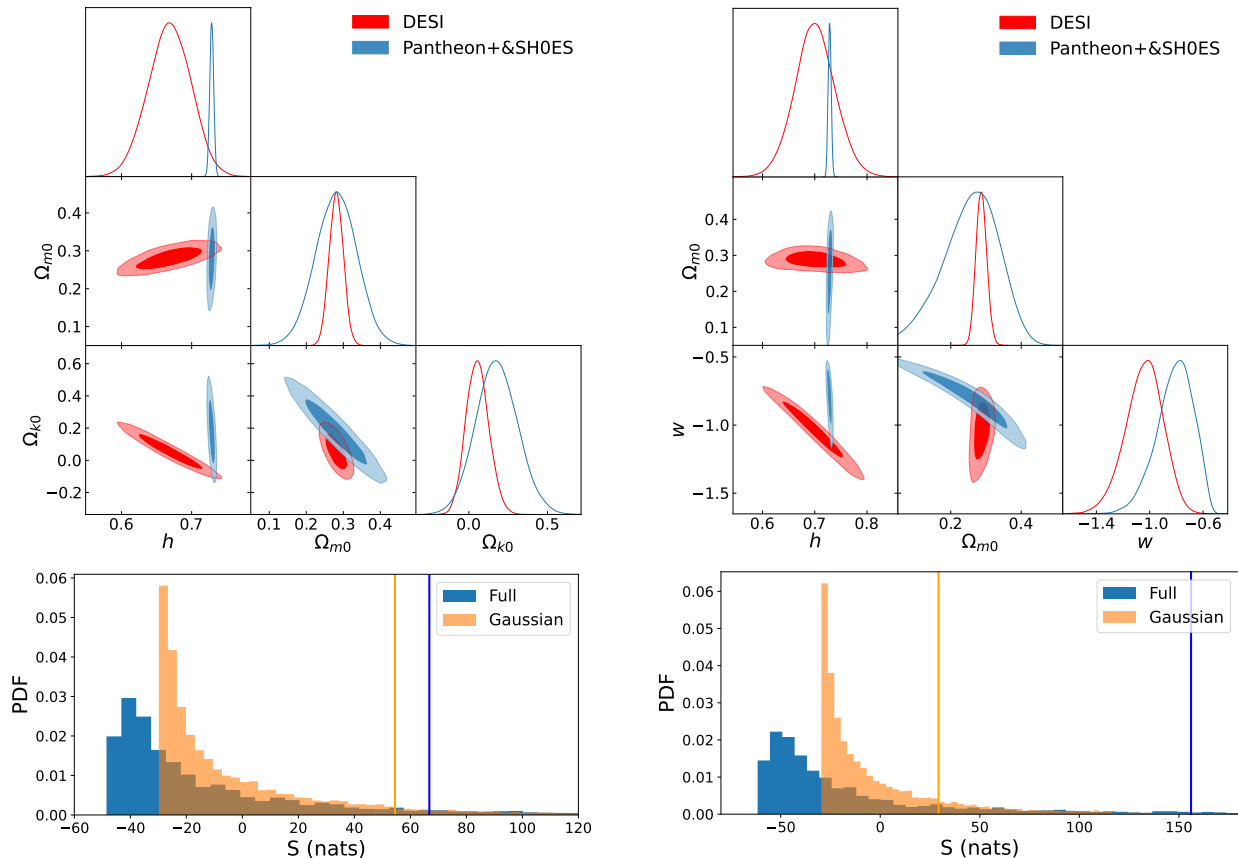


FIG. 8.— Similar to Figures 3 and 4 combined, but for the $\text{o}\Lambda\text{CDM}$ (left panel) and the $w\text{CDM}$ (right) models, and for the case where $\mathcal{D}_1 = \text{DESI}$ and $\mathcal{D}_2 = \text{Pantheon+ \& SH0ES}$. The blue and orange lines represent the value for the Surprise statistic in both its full form and its Gaussian approximation.

the non-Gaussian Surprise can successfully identify non-overlapping shapes in high dimensional space and point for discrepancies in data, which would otherwise be hidden using a Gaussian approximation with the full parameter covariance obtained with an MCMC chain.

We found that the non-Gaussian Surprise revealed a relevant 2.7σ tension between the Pantheon+ & SH0ES supernova data and the BOSS+ BAO + BBN data in the $\text{o}w\text{CDM}$ model. This tension, however, is completely hidden if one takes the Gaussian approximation for the surprise. Also, it is below 2σ in the smaller parameter space of the more restrictive models $\text{o}\Lambda\text{CDM}$, $w\text{CDM}$ and ΛCDM . For the comparison between Pantheon+ & SH0ES supernova data and the DESI BAO + BBN data, we find instead that the tension is below 2σ for the $\text{o}w\text{CDM}$, $\text{o}\Lambda\text{CDM}$ and $w\text{CDM}$ models, but around 3.3σ for ΛCDM . We find that the tension is primarily driven by discrepancies in the Hubble constant measurements.

For BAO data alone the Gaussian approximation gives reasonable results for the Surprise. For SNIa data instead, the Gaussian approximation is only accurate in the ΛCDM model. In the more general models, for which the parameters are less constrained, the distribution of the Surprise deviates significantly from its Gaussian solution, and the Gaussian Surprise fails to capture the full extent of the discordance when supernova data were included.

The full non-Gaussian surprise calculations with the `kl Surprise` code took around 500 CPU hours per pair of dataset, which is a very moderate computational cost. This means that for small parameter spaces one should perform the full calculations. In the future we plan to investigate how the code computational cost scales with a larger parameter space.

ACKNOWLEDGEMENTS

We thank Luca Amendola for useful discussions. PRM and MQ would like to express our sincere gratitude to Heidelberg University for their hospitality and support provided during our stay. MQ is supported by the Brazilian research agencies Fundação Carlos Chagas Filho de Amparo à Pesquisa do Estado do Rio de Janeiro (FAPERJ) project E-26/201.237/2022, CNPq (Conselho Nacional de Desenvolvimento Científico e Tecnológico) and CAPES (Coordenação de Aperfeiçoamento de Pessoal de Nível Superior). PRM is supported by the Brazilian research agency CAPES (Coordenação de Aperfeiçoamento de Pessoal de Nível Superior). BS is supported by Vector-Stiftung. We acknowledge the use of the computational resources of the joint CHE / Milliways cluster, supported by a FAPERJ grant E-26/210.130/2023.

REFERENCES

- Adame A. G., et al., 2024a, [2404.03000](#)
Adame A. G., et al., 2024b, [2404.03002](#)
Aghamousa A., et al., 2016, [1611.00036](#)
Alam S., et al., 2017, MNRAS, 470, 2617, [1607.03155](#)
Alam S., et al., 2021, Phys. Rev. D, 103, 083533, [2007.08991](#)
Amendola L., Marra V., Quartin M., 2013, MNRAS, 430, 1867, [1209.1897](#)
Amendola L., Patel V., Sakr Z., Sellentin E., Wolz K., 2024, [2404.00744](#)
Aubourg E., et al., 2015, Phys. Rev. D, 92, 123516, [1411.1074](#)
Beutler F., Blake C., Colless M., Jones D. H., Staveley-Smith L., Campbell L., Parker Q., Saunders W., et al., 2011, MNRAS, 416, 3017, [1106.3366](#)
Bhattacharyya A., 1946, Sankhyā: The Indian Journal of Statistics (1933-1960), 7, 401
Blas D., Lesgourgues J., Tram T., 2011, J. Cosmol. Astropart. Phys., 2011, 034, [1104.2933](#), [ADS](#)
Bradbury J., Frostig R., Hawkins P., Johnson M. J., Leary C., Maclaurin D., Necula G., Paszke A., et al., 2018, JAX: composable transformations of Python+NumPy programs
Brout D., et al., 2022, ApJ, 938, 110, [2202.04077](#)
Burns A.-K., Tait T. M. P., Valli M., 2024, Eur. Phys. J. C, 84, 86, [2307.07061](#)
Campagne J.-E., Lanusse F., Zuntz J., Boucaud A., Casas S., Karamanis M., Kirkby D., Lanzieri D., et al., 2023, Open J. Astrophys., 6, 1, [2302.05163](#)
Castro T., Quartin M., 2014, MNRAS, 443, L6, [1403.0293](#)
Chevallier M., Polarski D., 2001, Int. J. Mod. Phys. D, 10, 213, [gr-qc/0009008](#)
Cortés M., Liddle A. R., 2024, [2404.08056](#)
Cyburt R. H., Fields B. D., Olive K. A., Yeh T.-H., 2016, Rev. Mod. Phys., 88, 015004, [1505.01076](#)
de Sainte Agathe V., et al., 2019, A&A, 629, A85, [1904.03400](#)
Giesel E., Reischke R., Schäfer B. M., Chia D., 2021, JCAP, 01, 005, [2005.01057](#)
Golshani L., Pasha E., 2010, Information Sciences, 180, 1486
Grandis S., Rapetti D., Saro A., Mohr J. J., Dietrich J. P., 2016, MNRAS, 463, 1416, [1604.06463](#)
Grandis S., Seehars S., Refregier A., Amara A., Nicola A., 2016, JCAP, 05, 034, [1510.06422](#)
Handley W., Lemos P., 2019, Phys. Rev. D, 100, 043504, [1902.04029](#)
Heneka C., Marra V., Amendola L., 2014, MNRAS, 439, 1855, [1310.8435](#)
Higson E., Handley W., Hobson M., Lasenby A., 2018, Statistics and Computing, 29, 891–913, [1704.03459](#)
Hinshaw G., et al., 2013, ApJS, 208, 19, [1212.5226](#)
Hobson M. P., Bridle S. L., Lahav O., 2002, MNRAS, 335, 377, [astro-ph/0203259](#)
Hogg D. W., 1999, [astro-ph/9905116](#)
Huan X., Marzouk Y. M., 2013, Journal of Computational Physics, 232, 288–317
Kullback S., Leibler R. A., 1951, The Annals of Mathematical Statistics, 22, 79
Kunz M., Trotta R., Parkinson D., 2006, Phys. Rev. D, 74, 023503, [astro-ph/0602378](#)
Linder E. V., 2003, Phys. Rev. Lett., 90, 091301, [astro-ph/0208512](#)
Lindley D. V., 1956, The Annals of Mathematical Statistics, 27, 986
March M. C., Trotta R., Amendola L., Huterer D., 2011, MNRAS, 415, 143, [1101.1521](#)
Martin J., Ringeval C., Trotta R., Vennin V., 2014, Phys. Rev. D, 90, 063501, [1405.7272](#)
Nicola A., Amara A., Refregier A., 2019, JCAP, 01, 011, [1809.07333](#)
Pinho A. M., Reischke R., Teich M., Schäfer B. M., 2021, MNRAS, 503, 1187, [2005.02035](#)
Planck Collaboration VI 2020, A&A, 641, A6, [1807.06209](#)
Planck Collaboration XIII 2016, A&A, 594, A13, [1502.01589](#)
Planck Collaboration XV 2014, A&A, 571, A15, [1303.5075](#)
Raveri M., 2016, Phys. Rev. D, 93, 043522, [1510.00688](#)
Raveri M., Hu W., 2019, Phys. Rev. D, 99, 043506, [1806.04649](#)
Riess A. G., et al., 2022, Astrophys. J. Lett., 934, L7, [2112.04510](#)
Ross A. J., Samushia L., Howlett C., Percival W. J., Burden A., Manera M., 2015, MNRAS, 449, 835, [1409.3242](#)
Röver L., Bartels L. C., Schäfer B. M., 2023, MNRAS, 523, 2027, [2210.03138](#)
Sagredo B., Nesseris S., Sapone D., 2018, Phys. Rev. D, 98, 083543, [1806.10822](#)
Schöneberg N., 2024, JCAP, 06, 006, [2401.15054](#)
Schöneberg N., Lesgourgues J., Hooper D. C., 2019, JCAP, 10, 029, [1907.11594](#)
Schosser B., Mello P. R., Quartin M., Schaefer B. M., 2024, [2402.19100](#)
Schuhmann R. L., Joachimi B., Peiris H. V., 2016, MNRAS, 459, 1916, [1510.00019](#)
Scolnic D., et al., 2022, ApJ, 938, 113, [2112.03863](#)
Seehars S., Amara A., Refregier A., Paranjape A., Akeret J., 2014, Phys. Rev. D, 90, 023533, [1402.3593](#)
Seehars S., Grandis S., Amara A., Refregier A., 2016, Phys. Rev. D, 93, 103507, [1510.08483](#)
Sellentin E., Quartin M., Amendola L., 2014, MNRAS, 441, 1831, [1401.6892](#)
Skilling J., 2004, AIP Conf. Proc., 735, 395
Skilling J., 2006, Bayesian Analysis, 1, 833
Speagle J. S., 2020, MNRAS, 493, 3132, [1904.02180](#), [ADS](#)
Vargas-Magaña M., Brooks D. D., Levi M. M., Tarle G. G., 2018, in 53rd Rencontres de Moriond on Cosmology Unraveling the Universe with DESI, pp 11–18, [1901.01581](#)
Verde L., Protopapas P., Jimenez R., 2013, Phys. Dark Univ., 2, 166, [1306.6766](#)

APPENDIX

A. THE KLSURPRISE CODE

We built a python code to evaluate the Surprise distribution, a flow chart description of the code is shown in Figure 9. The code takes as input two main quantities, a python callable function of the posterior distribution $p(\Theta|\mathcal{D}_1)$ that takes as input a N_p -dimensional parameter vector Θ , and a python callable function for the likelihood of data 2, i.e. $\mathcal{L}(\mathcal{D}_2|\Theta)$. This function takes as

input two vector Θ , which is a d-dimensional parameter vector, and \mathcal{D}_2 which is a N-dimensional data vector. The code has two main routines, the `create_ppd_chain` and the `main_parallel` routine.

The `create_ppd_chain` routine is the first step into computing the Surprise distribution. It rewrites the PPD in Eq. (4) as in Eq. (5) and sample the distribution. The function takes as input a $\{N_s, d\}$ matrix, which we dub the Θ_M -matrix, containing the parameter samples $\{\Theta_i\}$ from the posterior distribution $p(\Theta|\mathcal{D}_1)$, where N_s is the number of samples of integral (5) and d is the dimensionality of the parameter space. The value for N_s is set

according to the preferred sampling method of the PPD. If one chooses to sample using an MCMC, N_s will depend on the convergence of the PPD, and can be taken to be 12000 for the BAO likelihoods. Another important parameter for the `create_ppd_chain` routine is the covariance matrix Σ_2 from likelihood function $\mathcal{L}(\mathcal{D}_2|\Theta)$.

The Θ_M parameter matrix can then be converted into a mock data matrix $\mathcal{D}_2^{\text{mock}}(\Theta)$ of dimensionality $\{N_s, N\}$, where N is the dimensionality of data space. This matrix is then used to build N_s likelihood functions $\{\mathcal{L}(\mathcal{D}_2^{\text{mock}}|\Theta)\}$ which are then used to sample the PPD distribution in Eq. (5). The sampling process can be done in two ways. If the dimensionality of data-space N is small enough, one can write Eq. (5) as a callable function of \mathcal{D}_2 and use any preferred sampling technique (such as MCMC or nested sampling). Else, if the dimensionality of data-space is prohibitively large, as in the case of a SNIa dataset, then one can randomly choose a subset of the mock likelihood functions $\{\mathcal{L}(\mathcal{D}_2^{\text{mock}}|\Theta)\}$. In this case, we assume them to be Gaussian, which for the case of a SNIa dataset is a reasonable assumption, sample the mock likelihoods and take all samples as the description of the PPD. Some tricks can be used to make the sampling process faster, such as Cholesky decomposition of the covariance matrix Σ_2 for instance. The samples of the PPD will induce the distribution of KLD.

The routine `main_parallel` takes a matrix of dimensionality $\{N_{\text{ppd}}, N\}$, where N_{ppd} is the number of PPD samples and each line of size N is a PPD sample. N_{ppd} has to be large enough to ensure a good resolution of the surprise p -value, and, in case the PPD sampling is performed with an MCMC or nested sampling technique, also large enough to ensure convergence of the sample. `main_parallel` returns a vector of N_{ppd} values for the KLD between the posterior constructed with each PPD sample of $\mathcal{D}_2^{\text{mock}}(\Theta)$ and the posterior distribution $p(\Theta|D_1)$. This function iteratively runs a Nested Sampling routine to estimate the posterior distributions from the i th entry of $\mathcal{D}_2^{\text{mock}}(\Theta)$, $p(\Theta|D_{2,i}^{\text{mock}})$, and then compute the value of KLD using Eq. (3). We use Nested Sampling to reconstruct the posteriors needed for computing the integral (3) (Skilling 2004, 2006), specifically the python Dynesty implementation (Speagle 2020). We make use of both the static and Dynamic Nested Sampling implementation (Higson et al. 2018) so we can properly sample the parameter space and get a good estimate of the evidence Z . The evidence estimation is a fundamental step into computing the value of KLD in Eq. (3), as both the posterior used must be normalized.

One could for instance try to avoid Nested Sampling altogether, use a preferred Monte Carlo technique to sample the posterior distribution and then estimate their normalized densities by means of a Kernel Density Estimator approach, but that will likely ultimately fail, as the reconstruction of the posterior distributions used in Eq. (3) must be also very accurate even in the regions with low posterior values, as these can be important when evaluating the numerical KLD of two disagreeing distributions.

The `main_parallel` routine will result in a vector $\{D_{\text{KL}}^i\}$ with N_{ppd} values for D_{KL} constructed with samples from the PPD. These are then used to reconstruct the distribution of KLD and consequently, the distribution of the Surprise. This routine is the main bottleneck

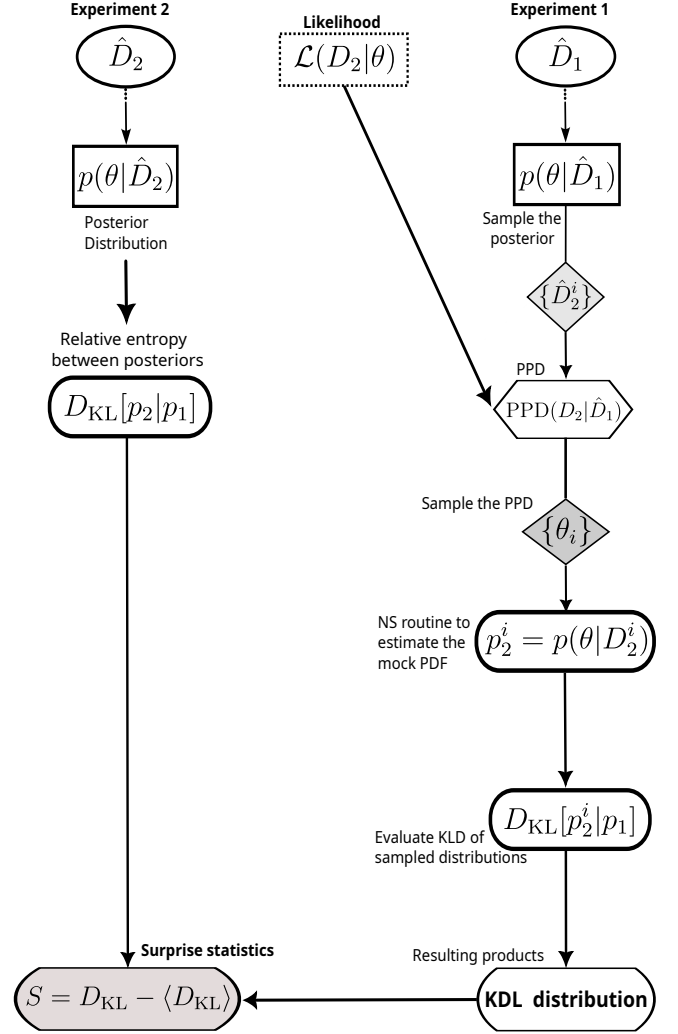


FIG. 9.— The main steps involved in evaluating the Surprise statistic distribution numerically.

of the code, as constructing the posterior distribution for each PPD sample is a time consuming process and scales accordingly to the dimensionality of parameter space and the efficiency of the Nested Sampling algorithm used. One can then use the routine `run_nested_sampling` and `compute_KLD_MCMC` to find the value of KLD between the two posterior distributions $p(\Theta|D_1)$ and $p(\Theta|D_2)$. Finally, the value of $\langle D_{\text{KL}} \rangle$ can be found by averaging the resulting vector of `main_parallel` $\{D_{\text{KL}}^i\}$. The Surprise is found by using Eq. (8) and its p -value is then evaluated from both S and its distribution. As the process of evaluating the distribution of S mixes a Bayesian and a Frequentist approach, the resulting p -value will have its error limited by the number of resulting samples in the Surprise distribution.

The most time consuming part of the code, to wit computing the KLD distribution, can be easily parallelized. We use `joblib` to distribute the computation of the different Nested Sampling runs needed to estimate $p(\Theta|D_2^i)$ for each PPD sample. With the reconstructed PPD mock posteriors, the integral in Eq. (3) can be easily vector-

ized by using Jax library (Bradbury et al. 2018). Sampling the PPD itself is not time consuming usually taking less than 1 minute for the quantities of samples we need. The plots in this paper were created with 5000 samples of KLD. For the case with $\mathcal{D}_1 = \text{BOSS+ \& BBN}$ and $\mathcal{D}_2 = \text{Pantheon+ \& SH0ES}$ the total computation time was 540 CPU hours (wall time around 11h in our 50-core workstation). If we consider a different scenario with $\mathcal{D}_1 = \text{BOSS+}$ and $\mathcal{D}_2 = \text{DESI}$ the computational times shrink significantly, with the whole code taking about 71 CPU hours (wall time around 1h30). Ultimately, the

run times will vary significantly depending also on the likelihood used and its implementation. It will increase linearly with the number of points one needs for the D_{KL} distribution.

This paper was built using the Open Journal of Astrophysics L^AT_EX template. The OJA is a journal which provides fast and easy peer review for new papers in the **astro-ph** section of the arXiv, making the reviewing process simpler for authors and referees alike. Learn more at <http://astro.theoj.org>.